Intraductal papillary mucinous neoplasm of the pancreas rapidly xenografts in chicken eggs and predicts aggressiveness

Zhefu Zhao[1,2], Nathalie Bauer[1,2], Ewa Aleksandrowicz[1,2], Libo Yin[1,2], Jury Gladkich[1,2], Wolfgang Gross[1,2], Jörg Kaiser[2], Thilo Hackert[2], Oliver Strobel[2] and Ingrid Herr [ID][1,2]

[1] Section of Surgical Research and Molecular OncoSurgery, Heidelberg, Germany
[2] Department of General Surgery, University of Heidelberg, Heidelberg, Germany

Intraductal papillary mucinous neoplasm (IPMN) of the pancreas has a high risk of progressing to invasive pancreatic ductal adenocarcinoma (PDA), but experimental models for IPMN are largely missing. New experimental systems for the molecular characterization of IPMN and for personalized prognosis and treatment options for IPMN are urgently needed. We analyzed the potential use of fertilized chicken eggs for the culture of freshly resected IPMN tissue. We transplanted 49 freshly resected IPMN tissues into eggs and compared the growth characteristics to IPMN tissues transplanted into mice; this was followed by an analysis of histology, morphology, and marker expression. Of the IPMN tissues transplanted into eggs, 63% formed tumor xenografts within 4 days, while none of the 12 IPMN tissues transplanted into immunodeficient mice engrafted. In the eggs, the grafting efficiency of high-grade ($n = 14$) and intermediate-grade ($n = 17$) dysplasia was 77% and was significantly higher than the 39% grafting efficiency of low-grade dysplasia ($n = 18$). According to mucinous expression, 46 IPMN tissues were classified into gastric ($n = 6$), intestinal ($n = 3$), oncocytic ($n = 23$), and pancreatobiliary ($n = 14$) subtypes. The grafting efficiency was highest for the pancreatobiliary subtype (86%), followed by the oncocytic (70%), gastric (33%) and intestinal (33%) subtypes. The morphology and expression patterns of mucins, progression markers and pancreatic ductal markers were comparable between the primary IPMN tissues and their xenograft copies. The individual tumor environment was largely maintained during subtransplantation, as evaluated upon passage 6. This new IPMN model may facilitate experimental studies and treatment decisions for the optimal personalized management of IPMN.

Key words: IPMN of the pancreas, chorioallantoic membrane, xenograft models

Introduction

A clinical case report published by Ohashi in 1982[1] described for the first time intraductal papillary mucinous neoplasm (IPMN) as a "mucin-producing" pancreatic neoplasm. In the following decades, IPMN of the pancreas was considered a non-invasive epithelial neoplasm located in the pancreatic ducts and was characterized by mucus-producing papillae. Compared with ductal adenocarcinoma of the pancreas, IPMNs are less aggressive and have significant molecular differences.[2] Today, with the use of modern imaging techniques, IPMNs are more frequently diagnosed,[3–5] but IPMN still represents a complicated disease in terms of its diagnosis, classification, and management. Macroscopically, IPMNs are classified as "main duct IPMN" (MD-IPMN) and "branch duct IPMN" (BD-IPMN), or as "mixed duct IPMN" if both ducts are affected. According to the WHO subclassification of 2010, IPMNs are categorised into low-grade, intermediate-grade, and high-grade dysplasia and IPMN with associated invasive carcinoma.[6,7] Based on mucin expression and histological features, IPMNs are subgrouped into gastric, intestinal, pancreatobiliary and oncocytic IPMNs,[8–10] and this classification seems to be most suited for predicting prognosis.[11,12] An international consensus for the clinical management of IPMNs was published by Fukuoka in 2012, but there are concerns that these guidelines may not entirely achieve the optimal treatment.[13] For example, the suggested

What's new?

Intraductal papillary mucinous neoplasm (IPMN) is a dysplasia of the pancreas that often becomes invasive but studies of the noninvasive state are challenged by the lack of faithful model systems. Here the authors describe the successful establishment of three-dimensional IPMN xenografts from freshly resected patient tissue in chicken eggs. The egg xenografts reflected the malignancy and morphology of the primary tumor and may thus facilitate experimental studies, treatment decisions and optimal personalized management of IPMN.

treatment schedule for BD-IPMN high-risk precursor lesions,[14] or MD-IPMNs with a duct diameter between 5–9 mm may be underestimated.[15] These concerns are exemplified by the 5-year survival rate, which decreases from 90% to <50% when a non-invasive IPMN progresses to an invasive IPMN.[16,17] These uncertainties may be avoided by considering symptoms and diagnostic criteria as well as age, comorbidity, family history, and even cost factors.[18]

However, IPMN models for the detailed characterization and evaluation of potential chemopreventive agents are not commercially available. Reported IPMN cell lines are derived from only invasive IPMNs, and at least one of them progressed to pancreatic ductal adenocarcinoma (PDA) in culture.[19–21] Non-invasive human IPMN tumors hardly form tumors in mice and seem to grow solely in triple immunodeficient NOG mice, which are extremely expensive.[19] Therefore, new IPMN models are urgently needed to facilitate the molecular characterization of and decisions for the optimal treatment of individual IPMN subtypes.

We established an IPMN xenograft model in fertilized chicken eggs, which enabled a rapid xenograft formation within 4 days for 63% of freshly resected transplanted IPMN tissues, while the more aggressive types engrafted more efficiently. The xenograft tissue reflected the morphology and marker expression of the primary tissue in the patients. The tumor volume of well-growing, aggressive IPMNs could be enlarged by passaging, which enabled therapy experiments to be performed by the intraperitoneal (ip) injection of gemcitabine into the chick blood vessels.

Materials and Methods

Primary tumor cells

ASANPaCa cells were established from a human PDA from a patient in whom the invasive carcinoma developed from a IPMN precursor lesion. These IPMN-based cells were kindly provided by our colleague Dr. Nathalia Giese and cultured as described.[21]

Patient tissue

Freshly resected surgical samples were used. A fast transfer from the operation hall to our laboratory was enabled by the tissue bank (PancoBank) of our clinic, which takes responsibility for distribution, organization and preservation of freshly resected pancreas tissues for pathological diagnosis and research under the approval of the ethical committee of the University of Heidelberg and after written consent was

obtained from the patients (see 301/2001, S-407/2010, S-562/2012). The average size of tissue available for egg transplantation was around 15 × 15 mm and the size of every single IPMN tissue was documented. The diagnoses of tumor types were established using the conventional clinical and histological criteria of the World Health Organization (WHO).[22] In malignant tumors, tumor stages were defined according to the UICC guidelines.[23] All the surgical resections were indicated by the principles and practice of oncological therapy. Clinical pathologists determined the tumor types and the tumor stages according to the UICC guidelines for the classification of IPMNs.

Xenotransplantation of IPMN tissue into chicken eggs

Preparation of eggs. Fertilized eggs from genetically identical hybrid Lohman Brown (LB) chickens were obtained from a local ecological hatchery (Geflügelzucht Hockenberger, Eppingen, Germany). The eggs were delivered at Day 0 of chick development and were immediately cleaned with 70% warm ethanol. Then, the eggs were placed in a digital motor breeder (Type 168/D, Siepmann GmbH, Herdecke, Germany) at 37.8°C and 45–55% humidity with an activated turning mechanism to start Day 1 of the embryonic chick development. Four days after incubation, the turning mechanism of the incubator was switched off and a hole was cut into the eggshell to detach the embryonic structures from the eggshell by removing 3 ml albumin, from which 1–2 ml were injected back after inspection of the embryo. The hole was covered with Leukosilk® tape (BSN medical, Hamburg, Germany), and the eggs were incubated further with the turning mechanism switched off.

Preparation of freshly resected IPMN tissue. Freshly resected surgical IPMN specimens were transported in 5 ml Oncostore medium (Oncoscience AG, Wedel, Germany) on ice to the laboratory, where the necrotic tissue was removed. One quarter of each sample was embedded in Tissue Tek O.C.T. (Sakura, Zoeterwoude, The Netherlands) and stored at −80°C for future immunohistochemical analysis. The second quarter of the tissue was directly frozen in liquid nitrogen for future DNA or RNA analysis. The residual tissue was mechanically minced to 1–2 mm³ pieces with sterile scissors under laminar flow and in 500 μl Dulbecco's Modified Eagle's Medium (DMEM) (Sigma-Aldrich, Taufkirchen, Germany) containing 10% FCS (Sigma). After centrifugation, the tiny tumor pieces were digested in the freshly prepared digestion medium of 0.5 mg/mL collagenase II (Gibco

Thermo Fisher Scientific, Carlsbad, USA) in 5 ml DMEM/10% FCS at 37°C and in a humidified atmosphere of 5% CO_2 for 45 min to 2 hrs. After filtering with a 70-μm strainer (Sigma) and centrifuging, 500 μL of the digestion mix was gently mixed with Matrigel™ (BD Heidelberg, Germany) and seeded in 24-well plates. After 20 min of polymerization, 200 μl DMEM/10% FCS was added to each well followed by 5 to 7 days of culturing to obtain spheroid-like structures. In parallel, 200 μl of the supernatant was obtained after the minced IPMN tissue was centrifuged and transferred to another tube and mixed at a 1:1 ratio with Matrigel™.

Transplantation of primary IPMN tissue. Thermanox™ plastic cell culture coverslips (13 mm ø, Thermo Scientific, Rochester, NY, USA) were prepared by punching and enlarging the hole to a diameter of 9 mm using scissors. The rings were sterilized in 70% EtOH, followed by the placement of the dried rings on the chorioallantoic membrane (CAM) between days 9 and 11 of embryonic development. Then, the CAM inside the ring was gently scratched with a syringe needle to ensure the immediate blood supply to the xenotransplant. Spheroid-like structures and supernatant, both in Matrigel™, were pipetted at a volume of 50 μl to the scratched CAM regions on Day 9 of the development.

Serial transplantation of IPMN egg xenografts. For subtransplantation, the chicks were ethically euthanized at Day 18 of development, 3 days before hatching, as described.[24] The xenografts were resected, minced, and mixed 1:1 with Matrigel™, which was followed by the direct subtransplantation at a volume of 50 μl into freshly-prepared eggs on Day 9 of the development. Before passage 5, one of the tumor tissues was stored in dry ice and embedded in Tissue Tek O.C.T. compound (Sakura, Zoeterwoude, The Netherlands) for further analyses.

Evaluation of the engraftment, volume and latency. All the embryos that died before developmental Day 17 were excluded from further analyses. The engraftment rate was calculated using the following formula: $N1 \times 100/N2$ ($N1$ = number of embryos with a tumor; $N2$ = number of live embryos). The tumor volumes were determined after resection of the tumor xenografts using the following formula: Volume = $4/3 \times \pi \times r^3$ ($r = 1/2 \times$ square root of diameter 1 $\times$ diameter 2). The latency, defined as the time until tumor growth is visible, was documented.

Detection of in ovo *cell proliferation by BrDU-staining.* Hundred microliter of a 10 mg/mL solution of the thymidine analog 5-bromo-2′-deoxy-uridine (BrDU, BD Pharmingen, Heidelberg, Germany) were injected into CAM vessels of xenotransplanted eggs on Day 15 of development. The xenograft tissue was resected at Day 18. Tissue sections were fixed in 4% PFA, quenched with peroxidase and incubated with mouse mAb anti-BrDU, diluted 1:200 for 2 hrs. The signal was enhanced with the EnVision+ Kit HRP.Mouse.AEC+ (EnVision Systems (Agilent, Santa Clara, California, USA),
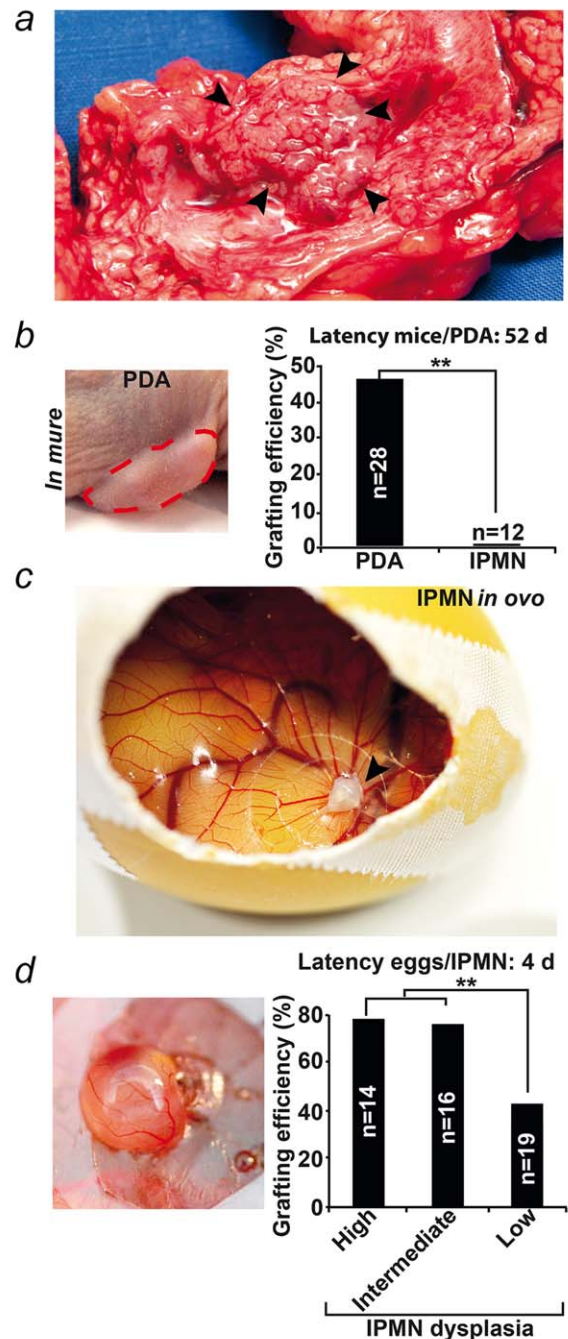
Figure 1. The IPMN grafting efficiency in eggs corresponds to histological grading. (*a*) A representative image of a pancreatic surgical specimen with a main duct IPMN (arrows). (***b***) Left: A representative photograph of a subcutaneous PDA xenograft in nude mice. Right: Twenty-eight freshly resected PDA tissues and 12 freshly resected IPMN tissues were subcutaneously transplanted into nude mice. The latency (days until tumor growth is visible) and grafting efficiency (percent of transplanted tissues that grew as xenografts) are shown as the mean values. *$p < 0.05$. (***c***) A representative photograph of an IPMN xenograft growing on the CAM of a fertilized chicken egg (arrow). (***d***) Left: The magnification of an IPMN xenograft *in ovo*. Right: The latency and grafting efficiency of 14 high-dysplasia, 16 intermediate-dysplasia and 19 low-dysplasia IPMN tissues that were transplanted into eggs were measured, and the mean grafting efficiency is shown. *$p < 0.05$. [Color figure can be viewed at wileyonlinelibrary.com]

Tumor Markers and Signatures

Table 1. Patient characteristics – IPMN tissues transplanted into mice and eggs

No.	Gender	Age	Morphological classification	Dysplasia	Sub-classification	MUC expression			Xenograft growth	
						1	2	5	*In ovo*	*In mure*
1	F	60	BD	Low	Oncocytic	+	−	−	✓	nd
2	F	63	BD	Low	Intestinal	−	+	+	✗	nd
3	F	73	MD	High	Oncocytic	+	−	−	✓	nd
4	M	65	MT	Low	Pancreatobiliary	+	−	+	✗	✗
5	M	52	BD	Low	Oncocytic	+	−	−	✗	nd
6	F	78	?	Intermediate	Pancreatobiliary	+	−	+	✓	nd
7	F	64	BD	Low	Oncocytic	+	−	−	✗	nd
8	M	57	BD	Intermediate	Pancreatobiliary	+	−	+	✓	✗
9	M	69	MD	High	Oncocytic	−	−	−	✓	nd
10	M	73	BD	Intermediate	Oncocytic	−	−	−	✓	✗
11	F	70	MT	High	Gastric	−	−	+	✓	nd
12	M	66	MT	High	Gastric	−	−	+	✓	✗
13	F	73	MT	Low	Gastric	−	−	+	✗	✗
14	F	70	MT	Intermediate	Oncocytic	+	−	−	✓	✗
15	M	64	MD	Low	Gastric	−	−	+	✗	✗
16	M	65	MD	Intermediate	Pancreatobiliary	+	−	+	✓	✗
17	F	57	BD	Low	Oncocytic	−	−	−	✓	✗
18	M	58	BD	High	Oncocytic	+	−	−	✓	nd
19	F	75	MT	Low	Pancreatobiliary	+	−	+	✗	✗
20	F	72	MT	Intermediate	Oncocytic	+	−	−	✗	nd
21	F	74	MT	Low	Oncocytic	+	−	−	✓	✗
22	M	66	MT	High	Oncocytic	−	−	−	✗	✗
23	M	67	MT	Intermediate	Gastric	−	−	+	✗	nd
24	M	74	MD	Intermediate	Pancreatobiliary	+	−	+	✓	nd
25	M	76	MT	High	Pancreatobiliary	+	−	+	✓	nd
26	M	61	MT	Intermediate	Oncocytic	+	−	−	✓	nd
27	F	59	MT	High	Oncocytic	+	−	−	✓	nd
28	M	69	MT	Low	Oncocytic	+	−	−	✓	nd
29	M	75	MT	Intermediate	Oncocytic	+	−	−	✗	nd
30	M	65	MT	Low	Intestinal	−	+	+	✓	nd
31	F	73	MT	Low	Gastric	−	−	+	✗	nd
32	M	49	BD	Intermediate	Pancreatobiliary	+	−	+	✓	nd
33	F	76	MT	Intermediate	Pancreatobiliary	+	−	+	✓	nd
34	F	73	MT	Intermediate	Pancreatobiliary	+	−	+	✓	nd
35	F	61	MT	Intermediate	Pancreatobiliary	+	−	+	✓	nd
36	M	37	MT	High	Pancreatobiliary	+	−	+	✓	nd
37	F	76	BD	Low	Intestinal	−	+	+	✗	nd
38	M	53	MD	High	Oncocytic	+	−	−	✓	nd
39	M	61	MD	Low	Oncocytic	+	−	−	✓	nd
40	M	58	MT	Intermediate	Pancreatobiliary	+	−	+	✓	nd
41	M	77	MT	Low	Pancreatobiliary	+	−	+	✓	nd
42	F	58	BD	Intermediate	nd	nd	nd	nd	✗	nd
43	M	62	MT	High	Oncocytic	−	−	−	✓	nd

Tumor Markers and Signatures

Table 1. Patient characteristics – IPMN tissues transplanted into mice and eggs (Continued)

| No. | Gender | Age | Morphological classification | Dysplasia | Sub-classification | MUC expression | | | Xenograft growth | |
						1	2	5	*In ovo*	*In mure*
44	M	64	MD	High	Oncocytic	+	−	−	✓	nd
45	F	73	MT	Low	nd	nd	nd	nd	✗	nd
46	M	81	MT	High	Oncocytic	−	−	−	✗	nd
47	F	65	BD	Low	nd	nd	nd	nd	✗	nd
48	F	62	?	High	Oncocytic	−	−	−	✗	nd
49	F	65	MT	Low	Oncocytic	−	−	−	✓	nd

Abbreviations: f: Female; **m**: Male; **IPMN**: intraductal papillary mucinous carcinoma; **Low**: low-grade dysplasia; **Intermediate**: intermediate grade dysplasia; **High**: high-grade dysplasia; **BD**: branch ductal; **MD**: main ductal; **MT**: mixed type; ✓: xenograft growth; ✗: no xenograft growth; **nd**: not done; **?**: unknown.

and the samples were counterstained with Hematoxylin-Eosin (H&E). H&E staining of IPMN xenografts from non-BrDU-injected eggs served as controls.

Xenotransplantation into immunodeficient mice

Surgically resected IPMN specimens from 12 patients and PDA specimens from 28 patients were minced, collagenase-digested, and mixed 1:1 with Matrigel[TM] as described above. A total of 300 μl of the mixtures was subcutaneously transplanted into the flanks of 6-week-old BALB c (nu/nu) immunodeficient mice, at 2 mice per tumor specimen. One to twelve months after transplantation, and depending on the engraftment, the mice were sacrificed and the percentage of tumor taken and latency were measured. The animal experiments were performed in the animal facilities of the University of Heidelberg after receiving approval from the authorities (Regierungspräsidium Karlsruhe, Germany).

Immunofluorescence for frozen tissue specimens

Frozen 6-μm tissue sections from the primary and xenografted tissues were fixed with 4% paraformaldehyde, and immunofluorescence staining was performed as recently described.[25] The following primary antibodies against human proteins were used: mouse monoclonal anti cytokeratin 19 (Abcam, Cambridge, UK), CD44 (BD/Pharmingen, Heidelberg, Germany), Mucin 1, Mucin 2, and Mucin 5AC (Thermo Fisher Scientific, USA), and KRAS (Abcam, Cambridge, UK), rabbit polyclonal anti Ki67 (Thermo Scientific, Rockford, IL, USA), CD24 (Santa Cruz, Heidelberg, Germany) and CxCR4 (GeneTex Inc., San Antonio, Texas, USA), goat polyclonal against c-Met (Biozol, Eching, Germany), SOX2 (Santa Cruz). Images were obtained using a Leica DMRB microscope and a SPOTTM FLEX 15.2 64Mp shifting pixel digital color camera.

Statistical evaluation

The significance of the differences between data sets was tested by a Student's t test, χ^2 test, Fisher exact test and Mann-Whitney test. A p values <0.05 was deemed to be statistically significant. One star represents $p < 0.05$, and two stars represent $p < 0.01$.

Results

The IPMN grafting efficiency in eggs corresponds to histological grading

For the establishment of the IPMN xenografts, we transplanted 12 freshly resected samples, including MD-IPMNs (Fig. 1), into the left and right flanks of BALB c (nu/nu) immunodeficient mice. The IPMN tumors were classified according to tumor location, WHO 2010 subclassification and mucin expression (Table 1) and reflected the diversity of the IPMN cases in terms of gender and age. However, no xenografts grew in the mice, even after transplantation of the 12th tissue and a 9-month waiting period (Fig. 1b). As an internal control, we compared against the engraftment rate of 28 freshly resected PDA tissues transplanted into mice and found that 46% (13/28) started to grow as xenografts within 52 days (Fig. 1b and Table 2), suggesting that our engraftment technique was not the reason for the failure of the IPMN tissue to form xenografts in these mice. To obtain a higher engraftment rate, we tried to inoculate freshly resected IPMN samples into the chorioallantoic membrane (CAM) of fertilised chicken eggs. This model resembles immunodeficient mice, because chick embryos are naturally immunodeficient and are an ethically justifiable and cheap alternative with less bureaucracy.[26,27] After transplantation of 49 IPMN samples into eggs, tumors grew from 31 (63%) of them within 3–4 days (Figs. 1c and 1d). The tumors had a three-dimensional structure and were well-supplied by the chick blood vessels. High-grade and intermediate-grade IPMNs had the best xenograft growth rates, which were 78% (11/14) and 76% (12/16), respectively, followed by a significantly lower tumor growth rate of 39% (11/19) for low-grade IPMNs. A total of 3 high-grade, 4 intermediate-grade and 11 low-grade IPMN tumors did not grow or grew and then subsequently receded. Depending on the amount of tissue transplanted and the proliferation rate, the xenografts had a volume between 20 and 200 mm^3.

Table 2. Patient characteristics from PDA tissues transplanted into mice

No.	Gender	Age	Grade	UICC stage	Xenograft growth
1	F	58	T1, N0 (0/22), G1, R0	1a	✗
2	M	64	T3, N1, G3, R1	2b	✗
3	M	45	T3, N1 (13/44), G2, R1	2b	✓
4	F	54	T3, N1 (3/20), G2, R1	2b	✓
5	F	23	T3, N1 (7/22), G3, R1	2b	✓
6	F	77	T1, N0 (0/17), G2, R0	1a	✗
7	M	58	T3, N1 (3/36), M1, R1	4	✗
8	F	75	T3, N1, M0, G3	2b	✗
9	M	63	T3, N1, M0, G3	2b	✗
10	F	70	Relapse	4	✓
11	F	61	T3, N1 (3/25), G3, R1	2b	✗
12	F	65	Peritoneal carcinomatosis	4	✗
13	F	61	T3, N1 (16/39), L1, G2	3	✗
14	M	79	T3, N1 (5/31), G3, R1	2b	✓
15	F	55	T3, N1 (6/39) G3, R1	2b	✓
16	M	51	T3, N1 (3/48), pM1, R1	2b	✓
17	F	53	T3, N1 (7/49), G3	2b	✗
18	M	52	Liver metastasis	4	✗
19	F	58	T3, N1 (5/24), G2, R1	2b	✓
20	M	59	T3, N1, G2	2b	✗
21	M	77	T3, N1, G2, R2	2b	✓
22	F	40	T3, N1 (16/30), G2, R1	2b	✓
23	F	63	T3, N1 (4/31), V1, G2, R1	3	✗
24	M	61	Liver metastasis	4	✓
25	M	63	T3, N1 (3/21), G2, R1	2b	✓
26	M	63	T3, N1 (1/13), M1, G2, R1	4	✗
27	M	71	T3, N1 (1/33), G2, R1	2b	✗
28	F	52	T3, N1 (11/24), G3, R1	2b	✓

PDA: pancreatic ductal adenocarcinoma; f: female; m: male; UICC: Union for International Cancer control; ✓: xenograft growth; ✗: no xenograft growth.

Egg xenografts mimic the morphology of the primary tumor of the patient

To determine whether the morphology of successfully engrafted xenografts resembles that of the primary tumor, we cryopreserved part of the tumor samples before and after xenotransplantation. H&E staining showed that the tumor grafts largely retained the major characteristics of the primary tumors, including ductal structures and fibrosis (Fig. 2a). Through immunofluorescence staining with human-specific antibodies and fluorescence microscopy, we found that the expression of some typical markers involving KRAS, cytokeratin 19, MHC, c-Met, CxCR4 and SOX2 was maintained in the egg xenografts, although the expression was weaker in some cases (Figs. 2b and 2c). This may be due to the infiltration of the tumor xenografts by the chick cells, most likely the chick fibroblasts, which form the tumor stroma. The chick cells are easily distinguishable from human cells, because they are smaller and not stained by the human-specific marker cytokeratin 19, but counterstained by DAPI.

The engraftment efficiency correlates to mucin expression

To analyse the association between xenograft growth and expression of the major mucin proteins Mucin 1, Mucin 2 and Mucin 5AC,[10] we stained sections from 46 patient tissues and the derived egg xenografts by immunohistochemistry; representative sections are shown (Fig. 3a). According to the mucin expression patterns, we classified the tissues into the gastric, intestinal, pancreatobiliary, and oncocytic subtypes, as described,[8–10] and compared the grafting efficiency of these subgroups. We found that pancreatobiliary and oncocytic IPMNs had higher engraftment efficiencies, which were 85% and 69%, respectively, compared to gastric IPMNs and

Tumor Markers and Signatures
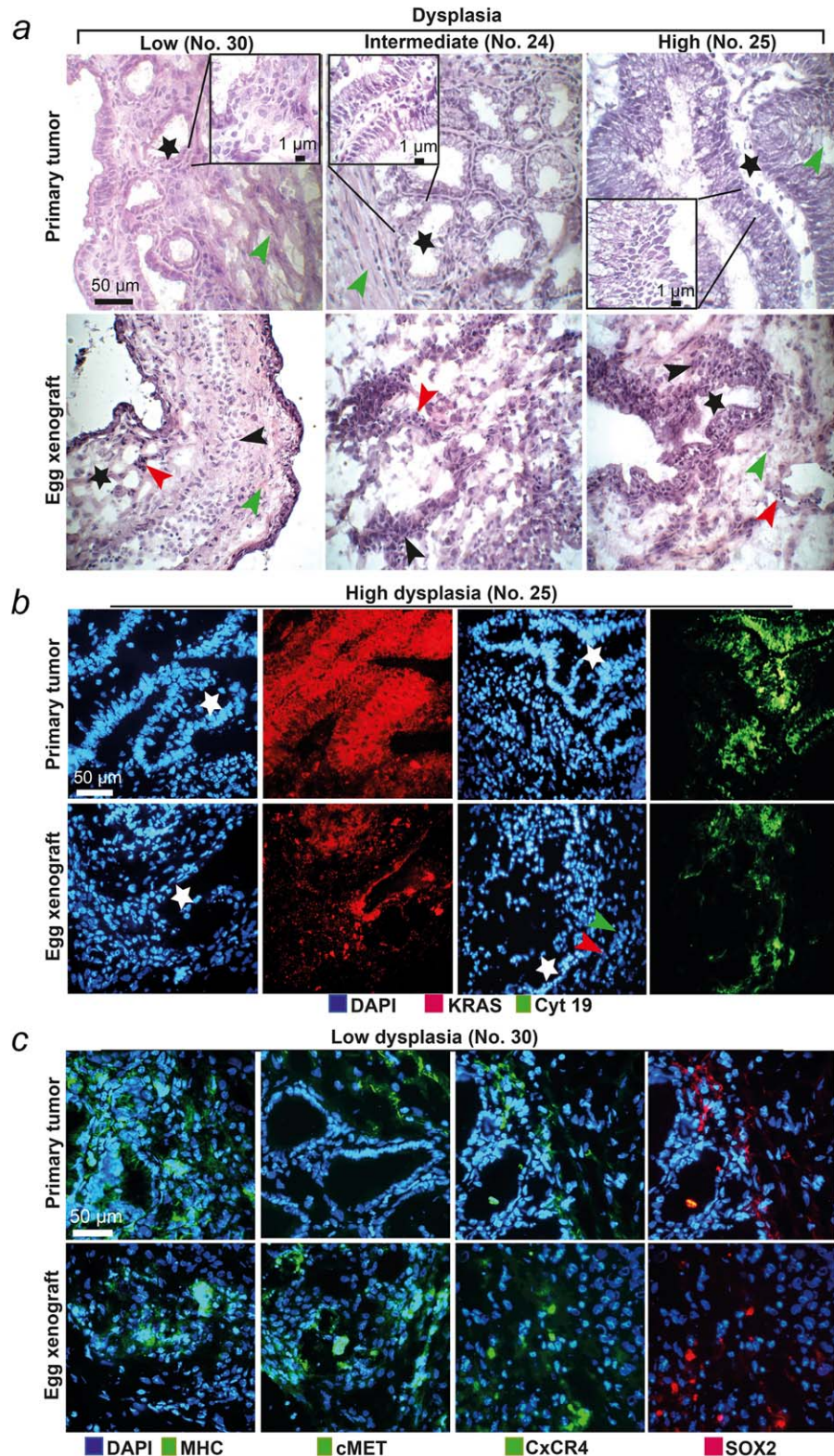
Figure 2. Egg xenografts resemble the primary patient tumor. (*a*) Representative images of H&E-stained primary tissue sections and the derived egg xenograft sections from a low-dysplasia (patient No. 30), intermediate-dysplasia (patient No. 24) and high-dysplasia (patient No. 25) IPMN. The sections were analyzed under 400× magnification. Asterisks: ductal structures; green arrows: tumor stroma/fibrotic regions; red arrows: chick cells; black arrows: human cells. (*b*) Representative images of immunofluorescence staining of primary tissue sections from a high-dysplasia IPMN (patient No. 25) and sections of the derived egg xenografts with KRAS (red) and cytokeratin 19 (Cyt19, green). The cell nuclei were stained with DAPI (blue). The sections were analyzed under 400× magnification. (*c*) Representative images of immunofluorescence staining of primary tissue sections from a low-dysplasia IPMN (patient No. 30) and sections of the derived egg xenografts with MHC, cMet, CxCR4 (green), and SOX2 (red). The cell nuclei were counterstained with DAPI (blue). The sections were analyzed under 400× magnification. [Color figure can be viewed at wileyonlinelibrary.com]
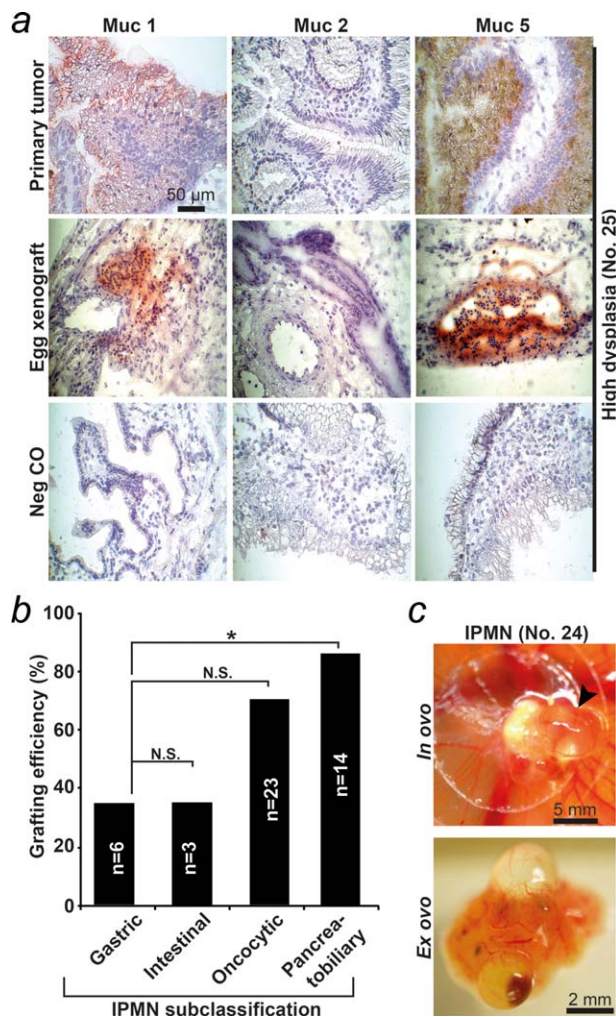
Figure 3. Tumor growth of IPMN in eggs correlates to mucin expression. (*a*) Representative images of immunohistochemistry stains of Mucin 1 (Muc 1), Mucin 2 (Muc 2) and Muc 5AC (Muc 5) in primary tumor sections from a high-grade dysplasia IPMN (patient No. 25) and tissue sections of the derived egg xenografts. Photographs were taken at 40× magnification. Stains without primary antibodies served as a negative control (Neg CO). (*b*) The grafting efficiencies of 6 gastric, 3 intestinal, 23 oncocytic and 14 pancreatobiliary IPMNs were measured by callipers, and the means are shown as percentages. *$p < 0.05$. N.S.: non-significant. (*c*) Representative images of a patient tumor-derived egg xenograft from an intermediate-grade dysplasia IPMN (patient No. 24) with mucinous sacs (arrows) *in ovo* (upper image) and after resection (*ex ovo*). [Color figure can be viewed at wileyonlinelibrary.com]

intestinal IPMNs, which each had engraftment efficiencies of 33% (Fig. 3*b* and Table 3). The higher grafting efficiency of pancreatobiliary IPMNs compared to gastric IPMNs was statistically significant, which corresponds to the reported grades of malignancies.[8–10] Interestingly, by macroscopic inspection and mucin staining, we detected "mucin sacs" in some IPMN xenografts (Fig. 3*c*). This finding supports our conclusion that the egg xenografts largely mimic the morphology and functional features of the primary IPMN tissues from patients.

Establishment of intravenous gemcitabine injection and serial transplantation on eggs using IPMN-derived ASANPaCa cells

According to the general opinion, the passaging of tumor xenografts in eggs is not possible,[28] and, to our knowledge, has never been described before—neither with established tumor cell lines nor with primary tumor tissue. To confirm, that cells are indeed proliferating on eggs, we xenotransplanted the IPMN-derived PDA cell line ASANPaCa cells to the CAM of fertilized chicken eggs and characterized the derived tumor xenografts by photography after resection and staining of xenograft sections by immunofluorescence and immunohistochemistry of CD44/CD24 and c-Met (Fig. 4*a*). Then half of eggs with xenotransplanted ASANPaCa cells were intravenously treated with gemcitabine (Fig. 2*b* left) or left untreated. Staining with the proliferation marker Ki67 and quantitative evaluation of positive cells revealed that many proliferating cells were present in the control xenografts and their number was significantly reduced by gemcitabine treatment (Fig. 4*b* on the right). Then, we tried serial transplantation, by mincing resected xenografts and re-transplantation to new eggs, which worked well (Fig. 4*c*) and is documented by pictures of representative xenografts on eggs of passages 1, 3 and 4, together with immunofluorescence stainings. Likewise, we measured the tumor volumes, which are presented as individual, mean and sum tumor volumes of each passage (Fig. 4*d*). By subtransplantation, we were able to increase the sum of tumor volumes from passage to passage.

Passaging on eggs enriches the tissue volume of aggressive IPMNs

Finally, we aimed to establish subtransplantation of freshly resected IPMN tissue on eggs to increase the available amount of xenograft tissue for treatment studies. Therefore, we subtransplanted IPMN tissue from a high-grade, intermediate-grade and low-grade dysplasia IPMN by passaging on eggs. The proliferation of IPMN on eggs was ensured by BrDU *in ovo* staining of xenografts in passage 4 from the high-grade IPMN (Fig. 5*a*). The number of the individual, mean and sum of tumor volumes of each passage up to 4 or 5 were obtained and are shown (Fig. 5*b*). While the mean volumes of high-grade and intermediate-grade dysplasia IPMNs increased, an increase in the total tumor volume was not obtained in the low-grade dysplasia IPMN. It should be noted that the number of tumors and the sum of tumor volumes would be even higher than what is shown because one xenograft from each passage was embedded for immunohistochemistry and is missing in the statistics. To predict the sensitivity of the different IPMN tissues to gemcitabine, we injected gemcitabine into those CAM blood vessels that supplied the tumor xenografts. Compared with the controls, which were injected with saline only, gemcitabine inhibited the mean tumor volume in the high-grade dysplasia IPMN

Tumor Markers and Signatures

Table 3. Sub-classification of IPMN specimens according to mucin expression

Morphological type	Histological type	Atypia	MUC1	MUC2	MUC5	Growth on eggs
			Mucin Expression			
MD ($n = 1$)	Gastric ($n = 6 = 13\%$)	Mild/low-grade	–	–	+	($n=2=33\%$)
Mixed ($n = 5$)						
BD ($n = 2$)	Intestinal ($n = 3 = 7\%$)	Moderate to severe/high-grade	–	+	+	($n=1=33\%$)
Mixed ($n = 1$)						
BD ($n = 2$)	Pancreatobiliary ($n = 14 = 30\%$)	Severe/high-grade	+	–	+	($n=12=85\%$)
MD ($n = 2$)						
Mixed ($n = 9$)						
BD ($n = 6$)	Oncocytic ($n = 23 = 50\%$)	Severe/high-grade	±	–	–[1]	($n=16=69\%$)
MD ($n = 5$)						
Mixed ($n = 11$)						

The expression of mucin 1 (MUC1), mucin 2 (MUC2) and mucin 5AC (MUC5) was determined by immunohistochemistry of 46 sections of primary IPMN tissue and the derived egg xenografts in passage 1. According to the mucin expression pattern and morphological classification, the IPMNs were grouped into the gastric, intestinal, pancreatobiliary, and oncocytic type.
Abbreviations: **BD**: Branch duct IPMN; **MD**: Main duct IPMN; **Mixed**: Mixed duct IPMN.

xenografts, whereas the effect was less pronounced in the intermediate-grade and low-grade dysplasia xenografts. Due to the small group sizes, we did not obtain statistically relevant data. Next, we stained sections of the primary IPMN of patient No. 25 and the derived egg tumor xenografts before and after gemcitabine treatment for the detection of morphology and CD44 and KRAS expression. Whereas the morphology of the egg xenograft resembled those of the primary tissue and typical duct structures are visible, gemcitabine treatment disturbed these structures. Also, both markers were expressed in the primary and xenograft tumor tissue, although the expression was weaker in 6th passage on eggs, and gemcitabine further eliminated the expression levels (Fig. 5c).

Discussion

In the present study, we validated the suitability of using fertilised chicken eggs for culturing freshly resected primary IPMN tissue. We found that 63% of the 49 transplanted IPMN tissues rapidly formed three-dimensional tumors in chicken eggs within 4 days. In contrast, none of the 12 IPMN tissues that we transplanted to BALB c (nu/nu) immunodeficient mice grew as a xenograft. Up to now, only two publications have successfully used immunodeficient mice for the transplantation of freshly resected IPMN tissue,[19,20] to our knowledge. One of them describes that 8 of 10 IPMN tissues grew in triple-immunodeficient NOG mice.[19] However, this was done at a four-times higher cost for NOG mice compared to BALB c (nu/nu) mice. From the available mouse xenografts, there are three established cell lines that could be used, but all the xenografts are derived from invasive IPMNs.[19,20] Therefore, a representative spectrum of IPMN cell lines or mouse xenografts from different pathological grades is not available. Our results suggest that this gap could be closed by IPMN xenografts in chicken eggs.

A major advantage of the egg xenograft model is its natural immunodeficiency because full immunocompetence develops only after hatching.[29] Xenografts are transplanted into the non-innerved but well-perfused CAM, which resembles the human placenta. Tumor tissue is usually transplanted into the eggs around Day 8 of embryonic chick development, when the blood vessel network of the CAM is dense enough to support xenograft growth. The egg xenografts have to be resected at Day 18, which is 3 days before hatching, because of the development of the immune response, nerve system and ethical reasons.[27,30,31] Therefore, the time span for xenograft growth is only 10 days, but this limitation may be compensated in part by the observed rapid engraftment within 4 days and the option of subtransplantation to new eggs. The xenotransplantation of IPMN tissue in chicken eggs can be easily performed in any laboratory, and this method is inexpensive and an animal application for approval by an ethics committee for animal experimentation is not required when the xenografts are resected and the chicks are euthanized at 18 of development in most countries.[27] In the UK researchers need a UK Home Office licence after Day 14 of development to do any work beyond Day 14.[26,32] Another limitation, compared to the mouse system, may be that birds are less genetically related to humans than are mice. However, the sequencing of the chicken genome revealed that the same number of genes is present as in humans, with high sequence conservation.[26] Moreover, the CAM is established for testing of tumor chemosensitivity[33,34] and a significant correlation was observed between LD50 cytotoxicity in rodents and eggs.[26,34,35]

The IPMN egg xenografts obtained in our study had a three-dimensional structure and were well supplied by chick blood vessels. The tumor morphology resembled that of the primary tissue, but was not identical, although clear ductal structures composed of human cells with enlarged, atypical nuclei were present in the xenografts. However, the density
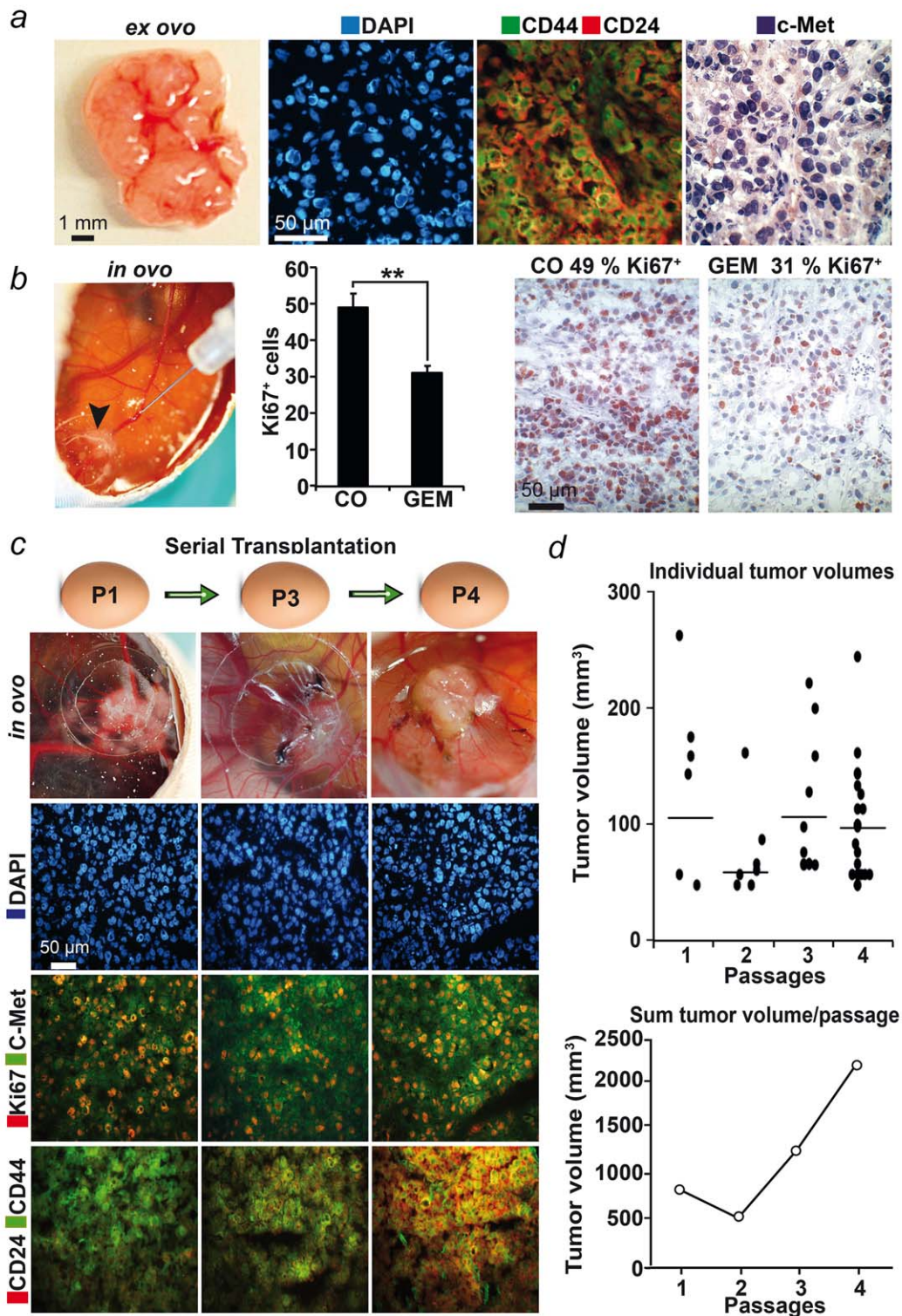
Figure 4. Establishment of intravenous gemcitabine injection and serial transplantation with IPMN-derived primary ASANPaCa PDA cells. (*a*) 5 × 10⁵ ASANPaCa cells were transplanted to the CAM of fertilized chicken eggs at Day 8 of embryonic development. Ten days later, the tumors were resected, and followed by double-immunofluorescence of frozen xenograft sections with CD44 (green)/CD24 (red) and counterstaining with DAPI (blue) or immunohistochemstry of c-Met. (*b*) The proliferation marker Ki67. The positive cells appear red to dark red. TGFβ-2 (green), E-cadherin (green), and vimentin (red) expression in xenograft sections was detected by immunofluorescence staining and the cell nuclei were counterstained with DAPI (blue). Cell sections were analyzed under 400× magnification, and representative images are shown. (*b*) ASANPaCa cells were transplanted to chicken eggs as described above and at Day 15 of development, half of the eggs were intravenously injected via CAM vessels (left picture, tumor xenograft is marked by an arrow) with 20 μL of a 10 μM gemcitabine (GEM) or were left untreated (CO). At Day 18, the tumors were resected and frozen tissue sections were stained with the proliferation marker Ki67 by immunohistochemistry. The number of positive cells was quantified in 10 visual fields at 400× magnification, and the means ±SD are shown. **p < 0.01. (*c*) Xenotransplanted ASANPaCa cells were resected at Day 18 of development, minced and re-transplanted to new eggs for 4 passages. The picture on the top is a cartoon of serial transplantation (P1: passage 1; P3: passage 3; P4: passage 4). Below, photographs of representative tumor xenografts growing on eggs at Day 17 are shown. Below, stainings of the resected tumor tissues with marker indicated are shown. (*d*) The tumor volumes of each individual tumor xenograft of each passage are presented as black dots and the mean tumor volume as black line. The diagram below shows the sum of tumor volumes of each passage. [Color figure can be viewed at wileyonlinelibrary.com]

of ductal structures, the grade of dysplasia, and the intensity of marker expression differed between primary tumor and egg xenografts and the egg tumor stroma was traversed by nests from chicken cells. One reason for this discrepancy may be due to mechanical mincing of the tissue before transplantation to eggs. Importantly, a typical pattern of mucin expression was maintained between the primary IPMN tissue and its egg xenograft, even after several passages of subtransplantation into eggs.

We used frozen IPMN specimens rather than formalin-fixed and paraffin-embedded tissues, because we found that fixing and embedding negatively influences the morphology of IPMN egg xenografts, which is most likely due to the presence of embryonic chick cells.

Interestingly, the ability of human IPMN tissue to grow in eggs was correlated to the grade of dysplasia because 78% of high-grade IPMNs and 76% of intermediate-grade IPMNs grew in eggs, whereas the engraftment rate of low-grade IPMNs was 39%, which is significantly lower. This difference was even more pronounced upon the subclassification of the IPMN specimens according to mucin expression. Here, the more malignant pancreatobiliary and oncocytic IPMNs grew in eggs at engraftment rates of 85% and 69%, respectively, which are significantly better than the mild to moderate aggressive gastric and intestinal IPMNs, which each had an engraftment rate of 33%. The data of the present study are confirmed by our unpublished work in which we transplanted 37 freshly resected PDA, 5 neuroendocrine tumours and 12 benign cystadenoma tissues to chicken eggs (Bauer and Herr 2017, in preparation for publication). A significant difference between the grafting efficiency of malignant and benign tissue was observed and the xenografts engrafted very fast within 2–4 days on eggs and the tumor morphologies and expression patterns of egg xenografts resembled those of the primary tumors, which was underlined by genomic expression profiling.
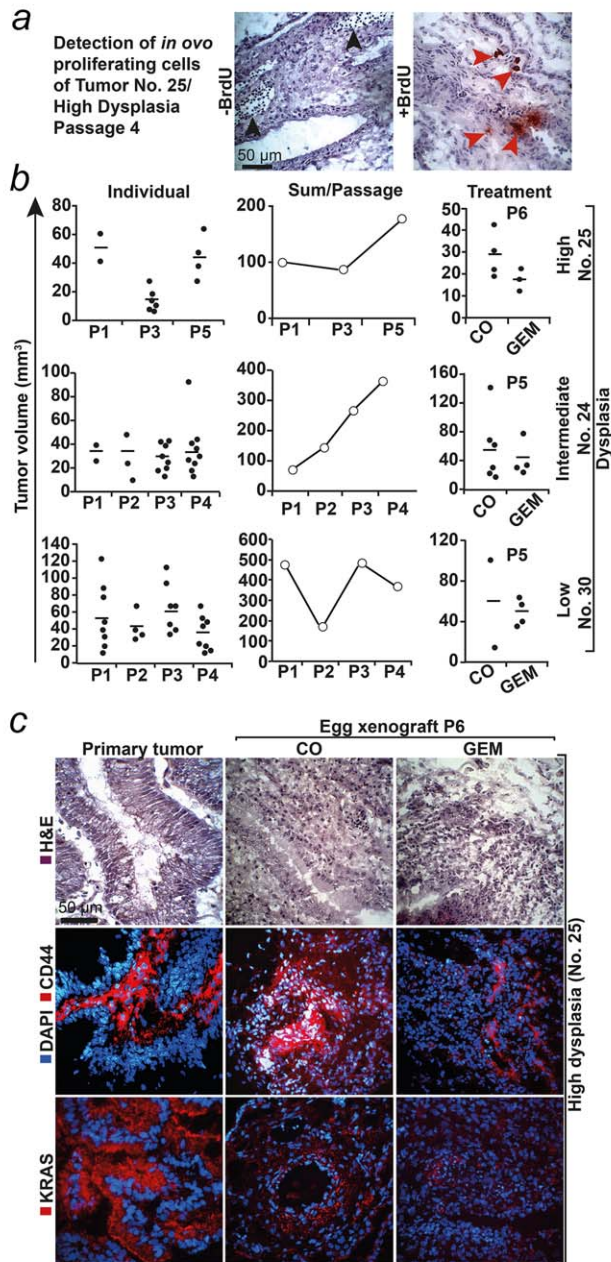

Figure 5. Serial transplantation enhances the volume of more aggressive IPMNs and enables treatment experiments. (*a*) Eggs harboring IPMN xenografts of primary tissue from high-dysplasia (patient No. 25) at passage 4 were injected with 100 μL of a 10 mg/mL BrDU solution at Day 15, followed by xenograft resection at Day 18. The presence of BrDU-positive, dividing cells (red arrows) was detected by immunohistochemistry and H&E counterstaining. IPMN xenografts of Patient 25 in passage 4 from non-BrDU injected eggs served as controls. (*b*) Serial transplantation of primary tissues from high-dysplasia (patient No. 25), intermediate-dysplasia (patient No. 24) and low-dysplasia (patient No. 30). P1: passage 1, P2: passage 2 and so on. The subtransplantations were repeated until, at passage 4 or 5, enough tumor xenografts for treatment experiments in small group sizes were available. Six days after transplantation, at passage 5 or 6, 50 μl gemcitabine (100 nM) was injected into the CAM blood vessels of the eggs from the treatment group (GEM), and saline was injected into the blood vessels of the control group (CO). Three days later, the xenografts were resected, the tumor volume was determined using callipers and the tissue was embedded in tissue Tek O.C.T. compound and stored on dry ice. The individual volumes of each tumor xenograft and the mean tumor volumes per passage are shown on the left (Individual). The sum of all individual tumor volumes from each passage is shown in the middle (Sum/Passage). The individual tumor volumes of untreated (CO) and gemcitabine-treated (GEM) eggs at passage 6 (No. 25) or passage 5 (No. 24 and No. 30) and the means are shown on the right. (*c*) Cryosections of primary tissue from a high-dysplasia IPMN from patient No. 25 and the derived xenograft tissue in passage 6, either treated with saline (CO) or gemcitabine (GEM) as described above, were stained with H&E or with specific antibodies to detect the expression of CD44 (red) and KRAS (red). The cell nuclei were counterstained with DAPI (blue). Representative images are shown under 400× magnification. [Color figure can be viewed at wileyonlinelibrary.com]

Figure 5.

This short grafting time of a relatively indolent tumor seems to be too short and difficult to reconcile with the dynamics of human disease. However, this very short grafting time is typical for egg xenografts and we also see it upon xenotransplantation of freshly resected pancreatic ductal adenocarcinoma or giant cell tumour of bone tissues.[36] The latter tumour entity may be comparable to IPMN, because it is semi-malignant and we confirmed by Alu *in situ* hybridization that indeed human tumour cells are present in the egg xenografts. We think that the fast engraftment and tumour growth on eggs is because of chick embryonic growth factors and a very good blood supply by vessels of the highly vascularized CAM. Most importantly, this very fast grafting may be seen as a big advantage compared to mouse xenografts, and both systems have different advantages and limitations. A limitation of the egg system may be that we were not able to receive by subtransplantation enough xenografts tissue for huge cohort treatment studies. We were only able to test gemcitabine efficacy with small group sizes ($n = 2$ to 6) and at one time point only. This issue has to be improved in future studies.

Therefore, the ability of a freshly resected IPMN tissue to form a tumor xenograft in fertilized chicken eggs may serve as an additional parameter for prognosis and supplement current prognosis models, such as the detection of KRAS and GNAS mutations in circulation[37,38] or pancreatic juice.[39,40] Importantly, IPMN egg xenografts derived from intermediate-grade dysplasia grew very well in eggs, at a rate that was comparable to that of high-grade IPMNs, suggesting that the current classification system may underestimate the aggressiveness of intermediate-grade IPMNs.

Conclusions

In summary, IPMN xenografts in chicken eggs are a promising tool for experimental and histological studies and may even be suited for complementing prognosis and the prediction of personalized therapy.

Declarations

Ethical approval and consent to participate

Acknowledgements

References

1. Ohashi KMY, Maruyama M, Takekoshi T, et al. Four cases of mucous-secreting pancreatic cancer. *Prog Dig Endosc* 1982;20:348–51.
2. Fritz S, Fernandez-del Castillo C, Mino-Kenudson M, et al. Global genomic analysis of intraductal papillary mucinous neoplasms of the pancreas reveals significant molecular differences compared to ductal adenocarcinoma. *Ann Surg* 2009;249:440–7.
3. Laffan TA, Horton KM, Klein AP, et al. Prevalence of unsuspected pancreatic cysts on MDCT. *AJR Am J Roentgenol* 2008;191:802–7.
4. Reid-Lombardo KM, St Sauver J, Li Z, et al. Incidence, prevalence, and management of intraductal papillary mucinous neoplasm in Olmsted County, Minnesota, 1984–2005. *A population study. Pancreas* 2008;37:139–44.
5. Simons JP, Ng SC, Shah SA, et al. Malignant intraductal papillary mucinous neoplasm: are we doing the right thing?. *J Surg Res* 2011;167:251–7.
6. Bosman FT, Carneiro F, Hruban RH, et al. WHO classification of tumours of the digestive system, 4th edn., vol. 3. WHO Press, 2010.
7. Castellano-Megias VM, Andres CI, Lopez-Alonso G, et al. Pathological features and diagnosis of intraductal papillary mucinous neoplasm of the pancreas. *Wjgo* 2014;6:311–24.
8. Furukawa T, Kloppel G, Volkan Adsay N, et al. Classification of types of intraductal papillary-mucinous neoplasm of the pancreas: a consensus study. *Virchows Arch* 2005;447:794–9.

9. Distler M, Kersting S, Niedergethmann M, et al. Pathohistological subtype predicts survival in patients with intraductal papillary mucinous neoplasm (IPMN) of the pancreas. *Ann Surg* 2013; 258:324–30.
10. Benzel J, Fendrich V. Molecular Characterization and Pathogenesis of Intraductal Papillary Mucinous Neoplasms of the Pancreas. *Eur Surg Res* 2015;55:352–63.
11. Adsay NV, Merati K, Andea A, et al. The dichotomy in the preinvasive neoplasia to invasive carcinoma sequence in the pancreas: differential expression of MUC1 and MUC2 supports the existence of two separate pathways of carcinogenesis. *Mod Pathol* 2002;15:1087–95.
12. Grutzmann R, Niedergethmann M, Pilarsky C, et al. Intraductal papillary mucinous tumors of the pancreas: biology, diagnosis, and treatment. *Oncologist* 2010;15:1294–309.
13. Tanaka M, Fernandez-del Castillo C, Adsay V, et al. International consensus guidelines 2012 for the management of IPMN and MCN of the pancreas. *Pancreatology* 2012;12:183–97.
14. Strobel O. [Branch-duct IPMN: underestimated risk of malignancy]. *Chirurg* 2012;83:1084
15. Hackert T, Fritz S, Klauss M, et al. Main-duct intraductal papillary mucinous neoplasm: high cancer risk in duct diameter of 5 to 9 mm. *Ann Surg* 2015;262:875–80. discussion 80-1.
16. Sohn TA, Yeo CJ, Cameron JL, et al. Intraductal papillary mucinous neoplasms of the pancreas: an

updated experience. *Ann Surg* 2004;239:788–97. discussion 97-9.
17. Salvia R, Fernandez-del Castillo C, Bassi C, et al. Main-duct intraductal papillary mucinous neoplasms of the pancreas: clinical predictors of malignancy and long-term survival following resection. *Ann Surg* 2004;239:678–85. discussion 85-7.
18. Goh BK. International guidelines for the management of pancreatic intraductal papillary mucinous neoplasms. *WJG* 2015;21:9833–7.
19. Kamiyama H, Kamiyama M, Hong SM, et al. In vivo and in vitro propagation of intraductal papillary mucinous neoplasms. *Lab Invest* 2010;90: 665–73.
20. Fritz S, Fernandez-del Castillo C, Iafrate AJ, et al. Novel xenograft and cell line derived from an invasive intraductal papillary mucinous neoplasm of the pancreas give new insights into molecular mechanisms. *Pancreas* 2010;39:308–14.
21. Heller A, Angelova AL, Bauer S, et al. Establishment and characterization of a novel cell line, ASAN-PaCa, derived from human adenocarcinoma arising in intraductal papillary mucinous neoplasm of the pancreas. *Pancreas* 2016;45:1452–60.
22. Bosman FT, Carneiro F, Hruban RH, et al. WHO Classification of Tumours of the Digestive System, 4th ed., vol. 3: WHO Classification of Tumours, 2010.
23. Brierley JD, Gospodarowicz MK, Wittekind C. UICC: The TNM Classification of Malignant Tumours. 8th ed.: Wiley-Blackwell, 2016.

24. Aleksandrowicz E, Herr I. Ethical euthanasia and short-term anesthesia of the chick embryo. *Altex.* 2015;32:143–7.
25. Kallifatidis G, Rausch V, Baumann B, et al. Sulforaphane targets pancreatic tumour-initiating cells by NF-kappaB-induced antiapoptotic signalling. *Gut* 2009;58:949–63.
26. Ribatti D. The chick embryo chorioallantoic membrane (CAM) assay. *Reprod Toxicol.* 2017;70: 97–101
27. Institutional animal care and use committee (IACUC). Policy for use of avian embryos. https://www.brown.edu/research/sites/research/files/policies/avian-embryo-use-policy-and-notification-form.pdf, 2016.
28. Kaufman N, Kinney TD, Mason EJ, et al. Maintenance of human neoplasm on the chick chorioallantoic membrane. *Am J Pathol* 1956;32: 271–85.
29. Weber WT, Mausner R. Migration patterns of avian embryonic bone marrow cells and their differentiation to functional T and B cells. *Adv Exp Med Biol* 1977;88:47–59.

30. Ribatti D, Nico B, Vacca A, et al. The gelatin sponge-chorioallantoic membrane assay. *Nat Protoc* 2006;1:85–91.
31. Murphy JB. Transplantability of malignant tumors to the embryos of a foreign species. *JAMA* 1912;LIX:874
32. Home Office. Guidance on the operation of the animals (Scientific procedures) Act 1986. http://www.gla.ac.uk/media/media_313482_en.pdf, 2014.
33. Kunzi-Rapp K, Westphal-Frösch C, Schneckenburger H. Test system for human tumor cell sensitivity to drugs on chicken chorioallantoic membranes. *In Vitro Cell Dev Biol* 1992; 28A:565–6.
34. Zhang Y, Liu L, Fan P, et al. Aspirin counteracts cancer stem cell features, desmoplasia and gemcitabine resistance in pancreatic cancer. *Oncotarget* 2015;6:9999–10015.
35. Kue CS, Tan KY, Lam ML, et al. Chick embryo chorioallantoic membrane (CAM): an alternative predictive model in acute toxicological studies for anti-cancer drugs. *Exp Anim* 2015; 64:129–38.

36. Herr I, Sahr H, Zhao Z, et al. MiR-127 and miR-376a act as tumor suppressors by in vivo targeting of COA1 and PDIA6 in giant cell tumor of bone. *Cancer Lett* 2017;409:49–55.
37. Berger AW, Schwerdel D, Costa IG, et al. Detection of hot-spot mutations in circulating cell-free DNA from patients with intraductal papillary mucinous neoplasms of the pancreas. *Gastroenterology* 2016;151:267–70.
38. Kanda M, Knight S, Topazian M, et al. Mutant GNAS detected in duodenal collections of secretin-stimulated pancreatic juice indicates the presence or emergence of pancreatic cysts. *Gut* 2013;62:1024–33.
39. Wang J, Paris PL, Chen J, et al. Next generation sequencing of pancreatic cyst fluid microRNAs from low grade-benign and high grade-invasive lesions. *Cancer Lett* 2015;356:404–9.
40. Yu J, Sadakari Y, Shindo K, et al. Digital next-generation sequencing identifies low-abundance mutations in pancreatic juice samples collected from the duodenum of patients with pancreatic cancer and intraductal papillary mucinous neoplasms. *Gut* 2017;66:1677-87.

Tumor Markers and Signatures